by man, whose appearance should rather bear better preservation of varves, but it was natural effect of lake shallowing.

Chronology of laminated sediments above 7.34 m

The chronology of the sediment above 7.34 m, though based on varve counting, is significantly affected by the knowledge of calendar age of its older end, determined to 3211 cal BP (Goslar, Chapter 6.4). This age agrees, within limit of error, with the estimate based on varve counting. Fixing of both ends of the laminated sequence 3200 varves long, however, distinctly changes the estimate of age error within this sequence.

If the chronology is not fixed at its lower end, the error of age determined by counting varves from the top of sequence has a cumulative character and is distinctly asymmetric. This error, however, implements a general uncertainty of interpretation of disturbed sections. For example, the maximum positive error in the whole part of profile (+500 varves) corresponds to the maximum underestimation of varve number in all disturbed sections. If the chronology is fixed at both ends, the error of age depends on counting the varves both from the top and from the bottom. The change of age at any level requires thus the opposite corrections of varve counting below and above that level. Separately, both corrections may be allowed by the uncertainty of varve counting. However, the opposite simultaneous corrections in two fragments are less probable, since all disturbed sections were similar, and the varves were counted everywhere in the same manner. Therefore the error of chronology fixed at both ends is more symmetric and distinctly lower than the error of varve counting alone. Obviously, the age near one end of chronology is little dependent on varve counting from the second end. Both the error of varve counting and the error of age are dependent on quality of lamination, varying along the profile. The analytical calculation of age error in these circumstances is a very difficult problem, and it was estimated relying rather on the author's intuition than on strict calculations (Fig. 8.15). One may note that the error rises towards the middle of considered part of profile. The rate of rise at particular level is dependent on quality of lamination.

8.2. MINERALOGY AND GEOCHEMISTRY OF THE LAKE GOŚCIĄŻ HOLOCENE SEDIMENTS

Bożena Łącka, Ewa Starnawska, Michał Kuźniarski & Leszek Chróst

The mineral and chemical analysis of the Holocene deposits from the central part of Lake Gościąż was carried out on 52 samples representing six selected parts of the G1/87 sediment core. These parts of the Holocene profile correspond to the sedimentation during following intervals of calendar age: (1) 11,458 – 11,408; (2) 10,708 – 10,446; (3) 8596 – 8296; (4) 6534 – 6084; (5) 4061 – 3461; (6) 820 – -35 years BP, i.e. AD 1130 – 1985 (for chronological background see Goslar Chapter 8.1).

Mineral components of bulk and homogenized samples encompassing 10 varves were identified by XRD and DTA methods (Chapter 4.5). XRD identification of minor mineral components in the Holocene deposits was difficult due to the occurrence of amorphous and poorly crystallized hydroxides of Mn and Fe or/and the transformation products of the metastable authigenic minerals, and the high content of $CaCO_3$, up to 75%. Nevertheless, the variations in the content of the major authigenic minerals as well as terrigenous detritus allow us to state that these selected parts of the Holocene sediments represent six complexes with different mineral composition:

(1) 11,458 – 11,408 cal BP. The main mineral constituents of the lowest part of Holocene sediments are Mn, Ca, and Fe carbonates and Mn hydroxides. Within the carbonate group, Ca-rhodochrosite predominates over calcite, siderite, and kutnahorite. These sediments, like the Younger Dryas deposits, may be regarded as Mn ores.

(2) 10,708 to 10,446 cal BP. Within the sediments formed during this time interval, the increase of calcite content was observed. This mineral becomes more abundant than Mn and Fe carbonates. Mn mineral phases other than carbonate displayed on the diffraction patterns are pyrolusite and todorokite.

(3) 8596 to 8296 cal BP. Mn and Fe carbonates decrease to the trace level. The main mineral components recorded in the diffraction patterns are calcite and gypsum. In this sequence of sediments vivianite appears to be another mineral phase of iron. Because of the high content of calcite the sediments from the third complex can be classified as carbonate gyttja.

Gypsum was recorded in the diffraction patterns of all samples investigated from Younger Dryas to recent, but within the carbonate gyttja that formed during the interval from 8596 to 6084 cal BP (complexes nos. 3 and 4) gypsum may be considered as one of the major mineral components of gyttja. The combined EDS and SEM analyses indicate that gypsum occurs more frequently within the light varve laminae. The morphology of gypsum crystals points to its late diagenetic origin.

(4) 6534 to 6084 cal BP. Sediments show the mineral composition similar to that of the underlying carbonate gyttja. The only exception is the occurrence of pyrite. In this part of the core two Fe-containing minerals, vivianite and pyrite, were X-ray detected.

(5) 4061 to 3461 cal BP. The mineral composition of the sediments is similar to that of the sediment complex no. 4. There occur two Fe-containing mineral phases, sulfides and phosphates. Pyrite and vivianite were undoubtedly identified by means of X-ray diffraction. The

difference in mineral composition between complexes no. 4 and 5 is a lower content of gypsum within the complex no. 5.

(6) 820 – -35 cal BP (AD 1130 – 1985). Gyttja from the uppermost part of the investigated Holocene sediment core is distinguishable by the high content of terrigenous detritus consisting of quartz, feldspar, layered aluminosilicates (mica, chlorite, and mixed-layer species), and rarely amphiboles. An abrupt increase in the quartz content can be observed within the gyttja sequence deposited after AD 1760, with two clear maxima corresponding to AD 1839, and AD 1940 – 1950. However, the lower part of this sequence, which contains only negligible amounts of quartz, is enriched in other detrital components, such as layered aluminosilicates and feldspar. The main authigenic component of this section of sediment is calcite. Iron minerals occur throughout the sequence. Siderite and ankerite were identified by XRD only within the parts of the sequence formed during the following time intervals: AD 1525 – 1590, AD 1875 – 1885, and AD 1940 – 1980. Pyrite occurs commonly within the whole sequence except for the interval AD 1920 – 1985. In samples from this interval lepidocrocite was identified. Fephosphates were difficult to reveal by means of X-ray diffraction owing to their poor crystallinity. Vivianite was detected in all tested samples. From all other iron phosphates recorded by means of the combined SEM and EDS analysis only cacoxenite was undoubtedly identified.

Varved sediments from Lake Gościąż that accumulated during the Holocene display the fine lamination varying in colour, thickness, composition, grain size, and cohesiveness as well. The laminae forming varves in the first and second analysed complexes show peculiar variety of colours. They are brown or beige to white. Texturally those laminae consist of resuspended carbonates and diatom frustules, suggesting sequential deposition of these components. The sequences and frequency of diatom laminae within the lowest part of the Holocene deposits suggest that seasonal plankton blooms were getting rare gradually, and most of diatom frustules were damaged and sunk in the carbonate matrix.

The third complex of sediments consists of varves in which the individual laminae show successive change in their colour, varying from almost black through reddish brown and beige to white. Usually thin and clearly defined black laminae are followed by wider, lighter, and more porous ones. The EDS analysis, made as maps of the element distribution in microarea (Fig. 8.16), demonstrated very close relationship between the laminae colour and the Mn, Fe, Ca, and P content. The dark laminae are composed of very fine carbonate grains and shapeless aggregates of Mn and Fe hydroxides (Plate 8.1, photos 1– 4). Carbonate grains consist of microcrystalline aggregates and irregular crystals. The subsequent laminae,

white and less porous, consist of almost pure calcite (Plate 8.1, photos 5, 6). The carbonate crystals are coarser there and more regular than those within beige laminae enriched in Mn and Fe hydroxides. The change in morphology of the carbonate crystals is probably connected to the presence of particulate or dissolved matter in the water column or/and pore waters. Such "impurities" may block the process of crystal growth. Euhedral and coarse calcite crystals crystallized probably under condition of low content of particulate and dissolved matter.

The enrichment in Fe phosphates was frequently observed within the darkest laminae. Fe phosphates occur in various morphological types of crystals (as radial aggregates and twinned plates; Plate 8.2, photos 1, 2) and lenticular amorphous clusters as well.

A distinct change of varves texture was observed in gyttja deposited from 6500 cal BP (complex no. 4). The varves of this complex are light-coloured, white, and pale grey, and they are composed of carbonate laminae differing from each other in porosity and grain size. Calcite crystals, regardless of grain size, are more euhedral there than those occurring within laminae with admixture of Mn and Fe hydroxides. SEM analysis shows that the growth of the crystal faces starts from a few nucleation
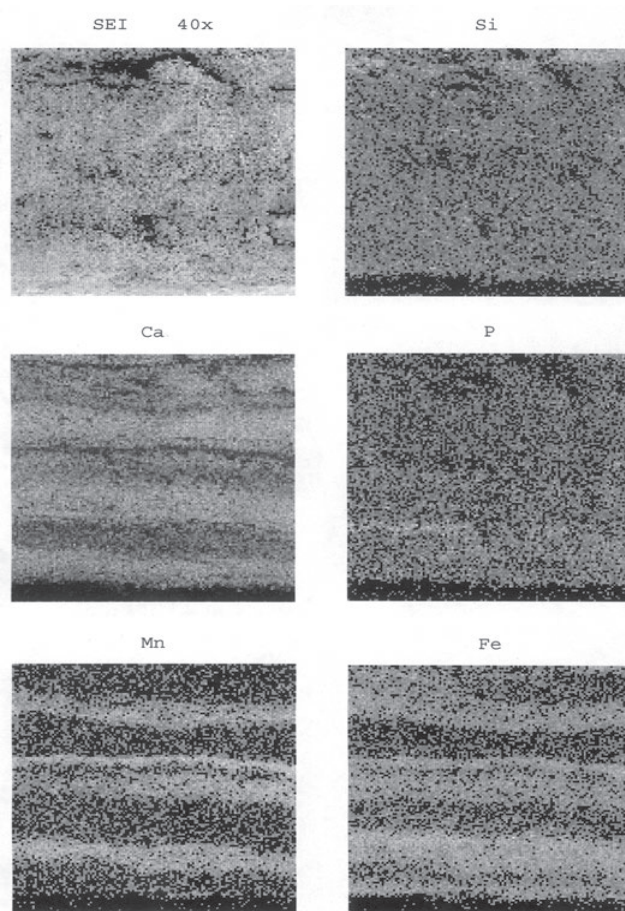

Fig. 8.16. Maps of secondary electron image (SEI) and element distribution within varves (complex no. 3).
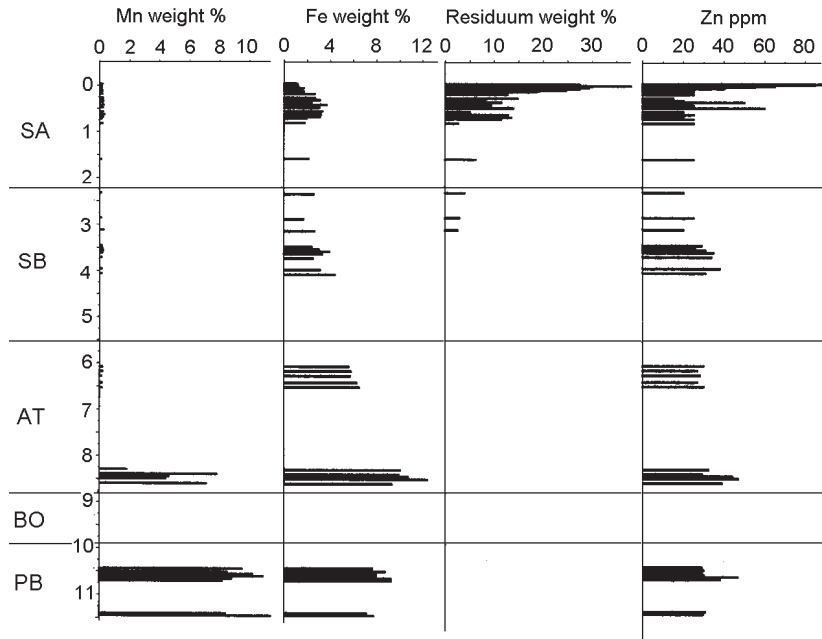
Fig. 8.17. The diagrams of Mn, Fe, acid-soluble residuum, and Zn variation versus time in kyr BP.

centres, and the pinholes within the crystal faces are filled afterwards. Finally, the crystals grow by building up successive bands on faces. Subsequently, growth of the deposited calcite crystals within the sediments results in building up {1010}, {1011}, and exceptionally {0112} crystal faces (Plate 8.2, photos 3–6).

In the uppermost part of the Holocene deposit, from 3000 cal BP, a gradual increase of diatom frustules has been observed, and distinct differentiation of diatom-rich

and diatom-poor laminae appeared. Maximum seasonal blooms of diatoms from AD 1861 have been reflected in the occurrence of laminae up to 0.5 cm thick, which are almost entirely composed of diatoms.

Framboidal pyrite has been found in sediments formed from 6000 cal BP to AD 1920. It occurs mainly as clusters of framboids on and/or within the carbonaceous organic remains (Plate 8.3, photos 1, 2).

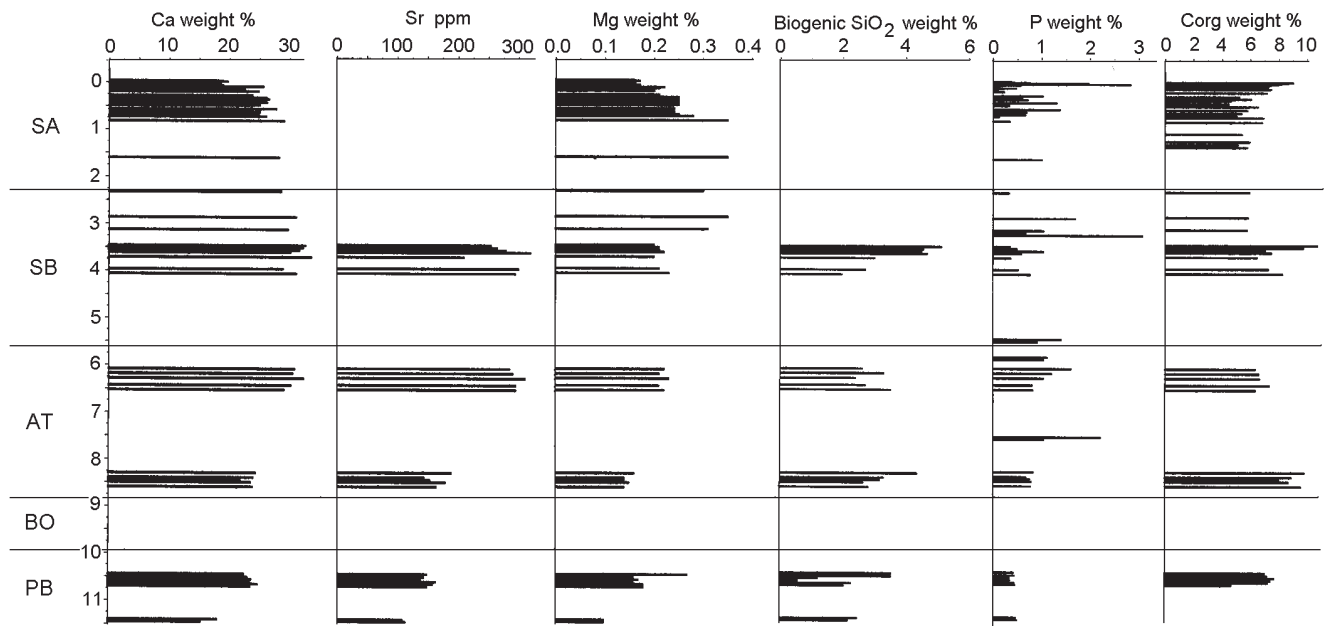Every one of analysed samples from G1/87 core rep-

Fig. 8.18. The diagrams of Ca, Sr, Mg, biogenic silica, phosphorus, and organic carbon variation versus time in kyr BP.

Table 8.2. Correlation coefficients for bulk and homogenized samples of the Holocene deposits (complexes nos. 1–5).

	Ca	Mn	Fe	SiO$_2$	Mg	K	Na	P	Sr	Zn
Ca	1									
Mn	-0.90	1								
Fe	0.03	0.14	1							
SiO$_2$	-0.51	0.26	-0.45	1						
Mg	0.85	-0.77	-0.11	-0.37	1					
K	-0.60	0.57	-0.18	0.40	-0.16	1				
Na	-0.03	0.13	0.17	-0.02	0.25	0.64	1			
P	0.46	-0.59	0.14	-0.15	0.40	-0.38	-0.10	1		
Sr	0.85	-0.93	-0.27	-0.25	0.82	-0.50	-0.18	0.58	1	
Zn	-0.14	0.23	0.27	0.08	-0.27	0.12	0.07	-0.20	-0.29	1

Table 8.3. Correlation coefficients for 1M HCl-dissolved fraction of bulk and homogenized samples of Holocene deposits (complex no. 6); Res = residuum, S$_{sulph}$ = sulphur from sulphate.

	Res	Fe	Mn	Ca	Mg	P	Zn	S$_{sulph}$	C$_{org}$
Res	1								
Fe	-0.73	1							
Mn	-0.58	0.86	1						
Ca	-0.96	0.68	0.51	1					
Mg	-0.93	0.55	0.43	0.91	1				
P	0.07	-0.03	0.02	-0.09	-0.02	1			
Zn	0.69	-0.65	-0.47	-0.71	-0.61	0.01	1		
S$_{sulph}$	-0.51	0.23	0.19	0.53	0.58	0.25	-0.20	1	
C$_{org}$	0.73	-0.79	-0.68	-0.77	-0.66	-0.17	0.76	-0.39	1

resents ten-year period of Holocene deposition in the central part of Lake Gościąż. Chemical composition of the deposits are presented in two sets of data: chemical composition of the bulk samples (complexes nos. 1 to 5), and chemical composition of 1M HCl-dissolved fraction of bulk samples (complex no. 6). In the first data set chemical composition of all mineral fractions is included, and the only exception is organic matter, which was not oxidized by HNO$_3$. The second set of data represents the chemical composition of acid-soluble components such as carbonates, phosphates, gypsum, iron monosulfides, and sulphates and Fe, Mn hydroxides, and oxides.

The relationship between elements is clearly shown by the values of correlation coefficients between them (Tabs 8.2 and 8.3). For bulk samples, Ca is highly and positively correlated with Mg and Sr. It suggests that these three elements are incorporated in the same mineral phase – calcite, the main Ca mineral of carbonates group. Mn and Fe are two other elements that can be incorporated into the carbonate structure. Nevertheless, the lack of positive correlation between Ca and Fe points to the occurrence of Fe in various mineral phases, not only carbonates. The high negative correlation between Ca and Mn is the effect of different mineralogy and the opposite trend of their accumulation throughout the Holocene profile.

Ca in the easily mobile fraction of sediment is highly and positively correlated with Mg. Similar high and positive correlation exists between Mn and Fe. This means that in the fraction of sediment that contains mainly the products of carbonate dissolution Mg is incorporated within the calcite structure and Mn mainly in siderite. Among other analysed elements, only Zn correlates negatively with all elements bound in carbonates.

Changes of chemical composition of sediments throughout Holocene as well as the variation of chemical composition between ten-year periods of sedimentation within selected complexes are presented in diagrams of element content versus time (Figs 8.17 and 8.18).

The Mn content (Fig. 8.17) shows the most significant change in the Holocene profile. From 6500 cal BP it decreases by two orders of magnitude (from 7–12% to 0.10–0.12%). The Mn content in sediments from the lower part of the Holocene profile (complexes nos. 1, 2) is very similar to that in the Younger Dryas deposits. Sediments from complex no. 3 are characterized by the gradual decrease of Mn concentration and by its high variation between samples representing ten-year periods of deposition.

The Fe distribution (Fig. 8.17) does not show such a sudden variation with time as that of Mn, but from 6500 cal BP the Fe content decreases from 8–12% to 2–7%.
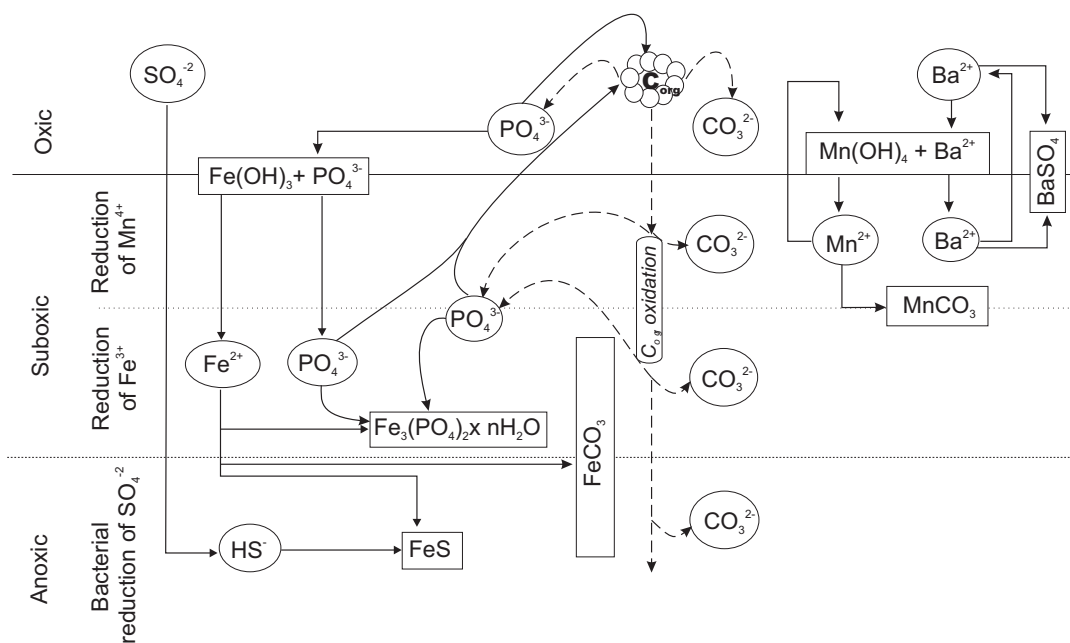
Fig. 8.19. Generalized distribution patterns of Mn, Fe, P, S, and Ba during early diagenesis of lacustrine deposits.

The maximum Fe concentration was found within sediments of complex no. 3, where it increased simultaneously with the distinct decrease in Mn content.

The variation of both elements is reflected in the change of the Mn/Fe ratio. The Mn/Fe ratio, about 1 in complexes nos. 1, 2, and 3, decreases to the value 0.02–0.03 for complex no. 4, becoming approximately equal to the Earth crust Mn/Fe ratio (Perelmann 1977). From 4000 cal BP, the sediments are characterized by the slightly higher and more differentiated Mn/Fe ratio, 0.05–0.10, but the Fe content is probably reduced due to the Fe determination in acid-soluble fraction only.

Because two different chemical procedures have been applied, the intervals with higher influx of clastic detritus are pointed out in two ways: (i) the distribution pattern of K and Na for the sediments formed during the interval 11,458–3461 cal BP, and (ii) distribution pattern of acid-insoluble residuum for the gyttja formed from 820 cal BP (Fig. 8.17). The variation of Na and K is negligible except for one sample (10,446 cal BP), where considerable increase in Na and K associated with the exceptional increase in Mg concentration was observed. Neither XRD nor SEM and EDS analyses show any differentiation of the mineral composition as compared to the underlying samples. However, these data can not exclude the presence of pyroclastic material within these sediments (Pawlikowski 1990).

Manganese and iron are easily mobile during the processes of sediment formation in lakes. The main source of these elements could be the matter delivered from land by surface and ground waters. The negligible content of terrigenous detritus excludes to some extent surface transportation. The variation of Mn/Fe ratio within sediments is probably the effect of weathering, depending on the climatic conditions and on the intensity of organic matter oxidation within the sediments and near the sediment/water column interface (Canfield et al. 1993, Dean et al. 1981, Egeberg et al. 1988, Schaanning 1988). In all these processes Mn is leached first and remains in solution longer than Fe. This is because Mn solubility exceeds that of Fe for any given Eh and pH range. The distribution of Mn and Fe within the Younger Dryas and lower part of the Holocene deposits (complexes nos. 1, 2, 3, 4) as well as the Mn/Fe ratio show a considerable enrichment in Mn and gradual increase in the Fe amount. It is suggested that these variations of Mn and Fe content are caused by the gradual change of climatic conditions, from subarctic to warmer and more humid (Borchert 1970, Crerar et al. 1971/72). A new Mn enrichment of the sediments was noticed in the upper part of the Holocene profile (complexes nos. 5 and 6), but this Mn enrichment is associated with the increase in the supply of clastic material. It could be a result of the lowering of the groundwater level and/or of the Eh decrease in near-shore environment. On the minor scale, the separation of Mn and Fe within sediments is shown on maps of element distribution within varve laminae (Fig. 8.16). This can be due to the redox condition within sediments. The surficial excess of manganese results from the continuous diagenetic recycling of the element within the sedimentary column. Upon burial in reducing condition, the dissolution of Mn can occur, and dissolved Mn can migrate upward and reprecipitate in relatively oxidizing environment near the sediment/water interface (Fig. 8.19).

The above-mentioned process is associated with the relative Fe enrichment of the sediments just below the

Mn-rich laminae, due to the immobilization of Fe in such mineral phases as hydroxides (oxidizing and slightly reducing condition), phosphates, monosulfides, and sulfides (reducing condition). The redox condition controlling the processes of the mobilization and mineral neoformation depend on the total amount of organic matter falling down. The increase of activity of anions released during the organic matter decay affects (i) the supply of nutrients to the water column and (ii) the pore-water saturation in respect to Fe and Mn mineral phases (phosphates, carbonates, and sulfides).

Distribution patterns of Ca, Mg, and Sr throughout the Holocene sediment profile show the same consistence of variation (Fig. 8.18) either in the bulk samples or in acid-soluble fraction. The fluctuation of their contents is influenced mainly by the oscillation of Mn content in the lower part of the Holocene deposits and the amount of the terrigenous detritus in the upper part.

The variation of biogenic silica, organic carbon, and phosphorus contents can be used to demonstrate the changes of bioproductivity in the lake. The distribution patterns of these components did not show clear differentiation between the separated complexes. However, biogenic silica as well as phosphorus contents are dif-

ferentiated between samples representing ten-year periods of sedimentation within the same complex (Fig. 8.19). Within complexes nos. 2, 3, and 5 the amount of biogenic silica increases towards the top of each complex, from 1 to 4 weight per cent (complex no. 2) and from 2 to 5 weight per cent (complex no. 5). The similar increase in the organic carbon was observed within the deposits of the complex no. 5, where C_{org} content rises from 8 to 12 weight per cent towards its top.

Slightly different distribution pattern is demonstrated by the variation of the P content with time (Fig. 8.18). Samples from complex no. 1 and 2 are depleted in P in comparison with the upper part of the Holocene profile (below 0.5 weight per cent). Upwards, P content rises to 1 weight per cent, on average. Nevertheless, one can also notice the occurrence of two maxima corresponding to 2–3 weight per cent of P (3218 cal BP and AD 1925–1950).

The greatest part of phosphorus in natural aquatic systems is derived from the oxidation of organic matter and recently from human activity (Emerson 1976, 1978, Jensen & Andersen 1992). Other natural sources of P, such as clay minerals, phosphatic bioclasts, and iron hydroxides, are of minor importance. Nevertheless, iron can control the geochemical migration of phosphorus in the
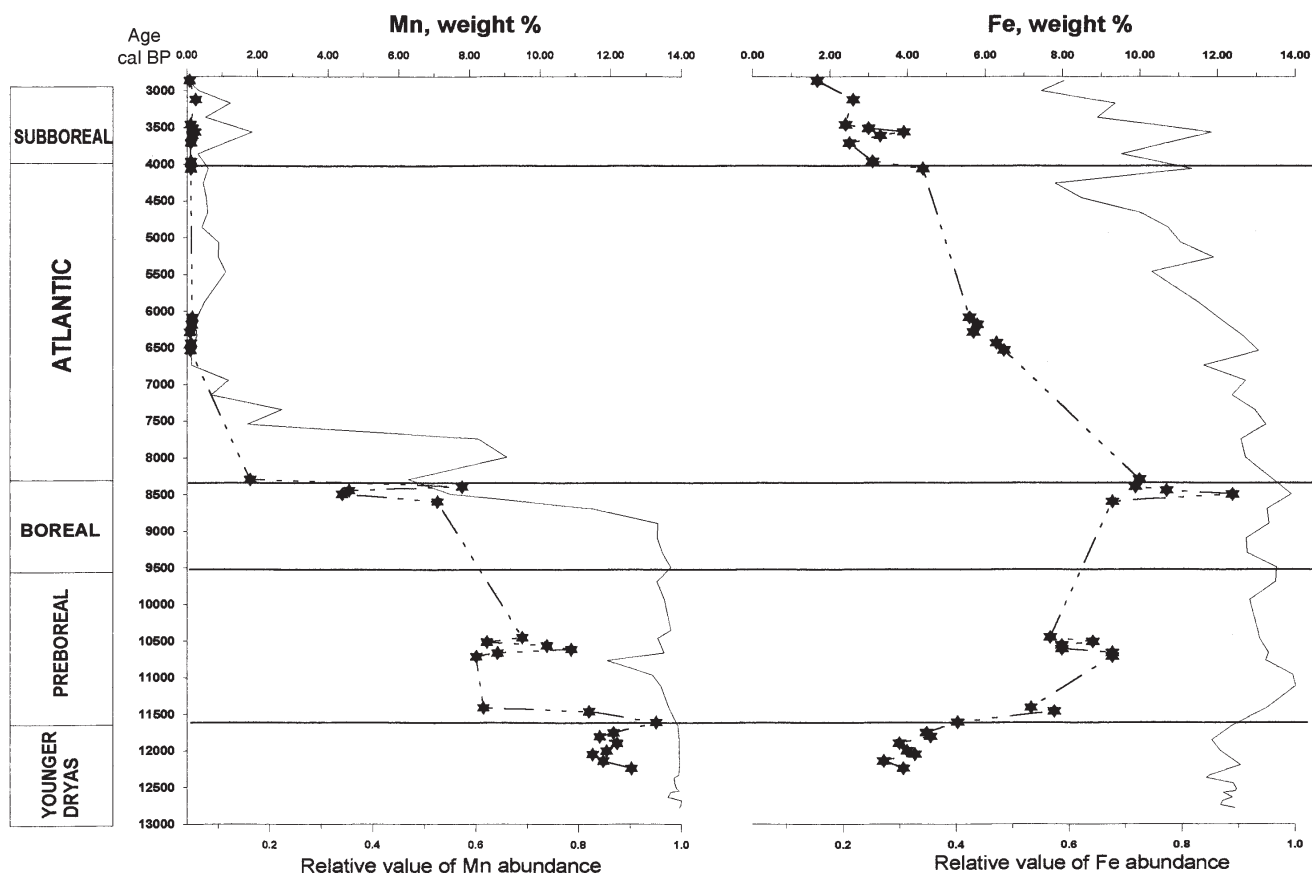

Fig. 8.20. The comparison of Mn and Fe distribution within the Lake Gościąż profile (stars – weight %) and the relative value of Mn and Fe within these deposits estimated by qualitative AAS method (line – data of L. Chróst).

freshwater environment wherever total iron is in large excess over sulphur. Particulate iron hydroxides strongly interact with dissolved species, depending on pH and local redox condition (Lucotte & d'Anglejan 1988). In oxic environment ferric iron oxides are the main scavenger of phosphate and trace elements (Fig. 8.19). The reductive dissolution of iron-containing compounds under reducing condition led to the release of the adsorbed P to the pore water (Martens et al. 1978, Sarazin et al. 1993, Tessier et al. 1985, Wersin et al. 1991) or to the direct precipitation of ferric-ferrous and ferrous phosphates (Buffle et al. 1989). Such annual recycling of P within the sediment column can influence the origin of Fe-phosphate-bearing laminae within a single varve. However, stagnant periods in the development of the lake followed by sediment disturbance can cause the anomalous large influx of phosphorus to the water column (Nriagu & Dell 1974), and thus it can control algal blooms.

The chemical data of the sediment samples from Lake Gościąż presented above should be consider as a preliminary investigation, giving only general trends of the geochemical changes during the evolution of the lake. Analyses were performed on few and small samples. Nevertheless, well-marked variations of the chemical composition that can be due to the climatic changes were noticed:

1. The two orders of magnitude decrease of Mn content from 6634 cal BP was preceded by two thousand years (from 8596 cal BP) of its gradual reduction. The interval of the abrupt Mn reduction within Lake Gościąż deposits may be further limited to 7500–7000 cal BP (Fig. 8.20), if we use the relative value of Mn abundance performed by L. Chróst.

The simultaneous decrease of the Mn/Fe ratio caused by the slight increase of Fe points to the change of the chemistry of particulate matter carried by the groundwater. This variation could arise from the gradual changes of the climate from subarctic to warmer and humid that resulted in the formation of a thick soil horizon.

2. The sediments formed from 8596 to 6634 cal BP are unusually enriched in iron. This may also be related to the climatic changes resulting in a eutrophic or/and a stagnant period of lake evolution. The setting up of reducing conditions at or near the bottom can prevent the Fe recycling within the sediment column, followed by the neoformation of Fe minerals (Marnette et al. 1993). The occurrence of pyrite as a main Fe mineral phase may be the consequence of the large influx of SO_4^{2-}– bearing waters to the bottom deposits.

3. Gypsum is one of the late diagenetic components of the sediments, and its maximum occurrence corresponds to the sediments originated from 8596 to 6634 cal BP.

4. The short events of P enrichment at 3218 cal BP and at AD 1925 could indicate periods of sediment disturbance preceded by stagnation of the lake system.

8.3. HOLOCENE REGIONAL VEGETATION HISTORY RECORDED IN THE LAKE GOŚCIĄŻ SEDIMENTS

Magdalena Ralska-Jasiewiczowa, Bas van Geel & Dieter Demske

The Gostynińskie Lake District, where Lake Gościąż is located, belongs genetically to the areas glaciated during the last cold stage. In the subdivision of Poland into the palaeoecological type regions (Ralska-Jasiewiczowa 1987, Ralska-Jasiewiczowa & Latałowa 1996), it has therefore been included to the Poznań-Gniezno-Kujawy Lake District as its easternmost part. However, as shown by recent pollen-analytical investigations, the vegetational development of the area reveals closer affinities with the central Masovian Lowlands. The best example of it is the pollen diagram from Lake Błędowo, situated in central lowlands ca. 100 km east of Lake Gościąż (Bińka et al. 1991), which, though very poorly dated by ^{14}C, is well correlated with the reference diagram from Lake Gościąż. This may be explained by the similar sandy subsoils, in contrary to the nearby Kujawy subregion, where black-earth (chernozem) soils dominate.

The Holocene vegetation history of the central Polish lowlands and adjacent lake districts, as now, has mostly been based on studies between the late 1950s and early 1980s (e.g. Oszast 1957, Kępczyński 1960, Borówko-Dłużakowa 1961a, Pyrgała 1972, Wasylikowa 1978, Jankowska 1980, Noryśkiewicz 1982). It also includes sites located very close to Lake Gościąż along the left bank of Vistula River, between Gąbin, Gostynin, and Włocławek (Borówko-Dłużakowa 1961b). The main deficiencies of those studies, however, is the poor time resolution in pollen diagrams and/or the lack of radiocarbon dates. The closest recently investigated sites meeting requirements of modern palaeoecology are
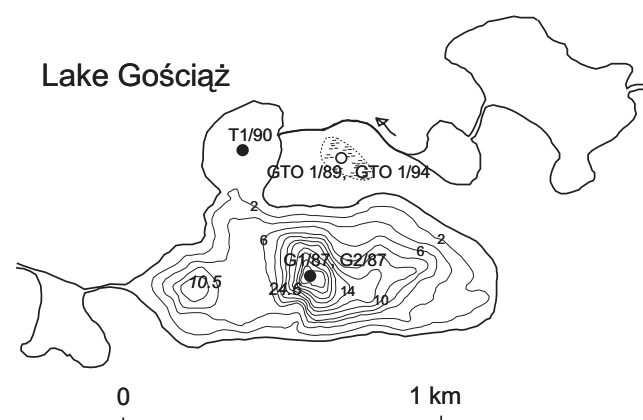

Fig. 8.21. Map of Lake Gościąż showing the location of profiles discussed in this chapter (black dots) and other Holocene profiles investigated by means of pollen and macrofossil analysis (white dot, Demske 1995).

Ralska-Jasiewiczowa M., Goslar T., Madeyska T. & Starkel L. (eds), 1998. Lake Gościąż, central Poland. A monographic study. Part 1.
W. Szafer Institute of Botany, Polish Academy of Sciences, Kraków.
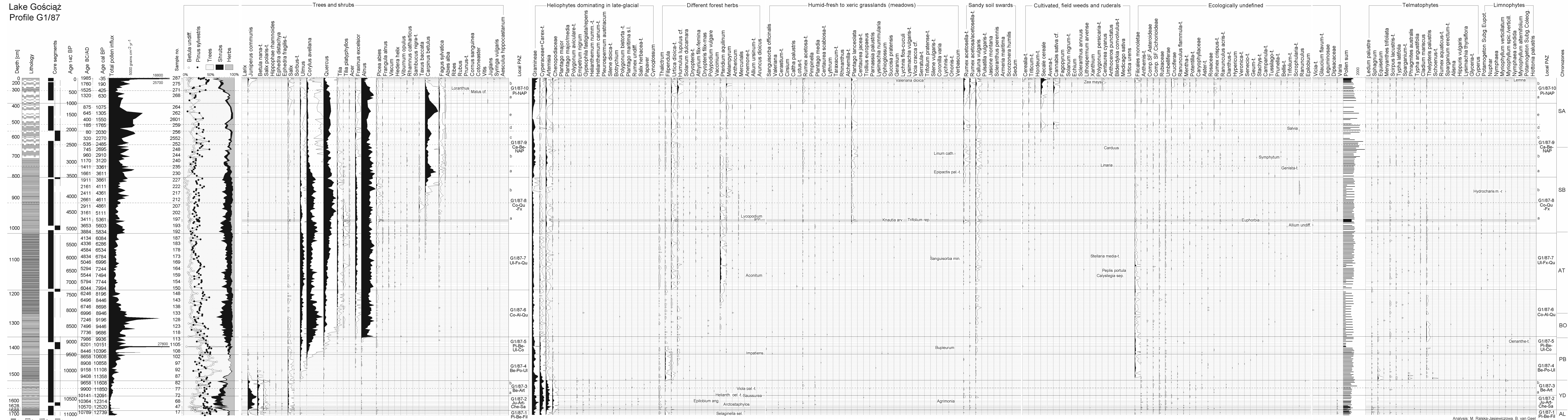
Lake Gościąż
Profile G1/87

Fig. 8.22. Lake Gościąż, profile G1/87, completed with the core sections from profile G2/87, both cores from the central lake deep – complete percentage pollen diagram. Parts of core segments indicated in black were sampled for pollen analysis. 1 – calcareous gyttja regularly laminated, 2 – calcareous gyttja, wavy laminae, 3 – calcareous gyttja, irregularly laminated, 4 – sand.
Because of some differences in pollen identification between both pollen analysts there are a few inconsistences in taxa nomenclature, e.g. *Tilia = Tilia* undiff., *Ramunculus = Ranunculus flammula* -t. + *R. acris* -t.

Analysis: M. Ralska-Jasiewiczowa, B. van Geel